Journal Pre-proofs

Identification of 5*H*-Chromeno[3,4-c]pyridine and 6*H*-Isochromeno[3,4-*c*]pyridine Derivatives as Potent and Selective Dual ROCK Inhibitors

Zilun Hu, Cailan Wang, Doree Sitkoff, Nathan L. Cheadle, Songmei Xu, Jodi K. Muckelbauer, Leonard P. Adam, Ruth R. Wexler, Mimi L. Quan

PII: S0960-894X(20)30585-0
DOI: https://doi.org/10.1016/j.bmcl.2020.127474
Reference: BMCL 127474

To appear in: *Bioorganic & Medicinal Chemistry Letters*

Received Date: 10 July 2020
Accepted Date: 4 August 2020

Please cite this article as: Hu, Z., Wang, C., Sitkoff, D., Cheadle, N.L., Xu, S., Muckelbauer, J.K., Adam, L.P., Wexler, R.R., Quan, M.L., Identification of 5*H*-Chromeno[3,4-c]pyridine and 6*H*-Isochromeno[3,4-*c*]pyridine Derivatives as Potent and Selective Dual ROCK Inhibitors, *Bioorganic & Medicinal Chemistry Letters* (2020), doi: https://doi.org/10.1016/j.bmcl.2020.127474

Graphical Abstract

Identification of 5*H*-Chromeno[3,4-*c*] pyridine and 6*H*-Isochromeno[3,4-*c*]pyridine Derivatives as Potent and Selective Dual ROCK Inhibitors

Leave this area blank for abstract info.

Zilun Hu,* Cailan Wang, Doree Sitkoff, Nathan L. Cheadle, Songmei Xu, Jodi K. Muckelbauer, Leonard P. Adam, Ruth R. Wexler, and Mimi L. Quan

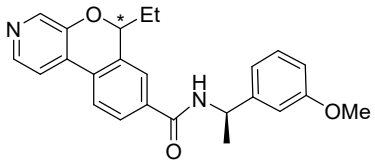

19
ROCK1 IC_{50} 0.67 nM
ROCK2 IC_{50} 0.18 nM
Kinome selectivity: FSI100 1.3

ELSEVIER

Bioorganic & Medicinal Chemistry Letters
journal homepage: www.elsevier.com

Identification of 5*H*-Chromeno[3,4-c]pyridine and 6*H*-Isochromeno[3,4-*c*]pyridine Derivatives as Potent and Selective Dual ROCK Inhibitors

Zilun Hu,* Cailan Wang, Doree Sitkoff, Nathan L. Cheadle, Songmei Xu, Jodi K. Muckelbauer, Leonard P. Adam, Ruth R. Wexler, and Mimi L. Quan

Research & Early Development, Bristol Myers Squibb, P.O. Box 5400, Princeton, New Jersey 08543-5400, USA

ARTICLE INFO

Article history:
Received
Revised
Accepted
Available online

Keywords:
Rho kinase
ROCK inhibitor
Chromenopyridine
Chromenopyrimidine

ABSTRACT

A novel series of 5*H*-chromeno[3,4-*c*]pyridine, 6*H*-isochromeno[3,4-*c*]pyridine and 6*H*-isochromeno[4,3-*d*]pyrimidine derivatives as dual ROCK1 and ROCK2 inhibitors is described. Optimization led to compounds with sub-nanomolar inhibitory affinity for both kinases and excellent kinome selectivity. Compound **19** exhibited ROCK1 and ROCK2 IC_{50} of 0.67 nM and 0.18 nM respectively.

* Corresponding author. Tel.: +1 609 252-6125; e-mail: zilun.hu@bms.com

serine-threonine protein kinase family. They are effector proteins of RhoA, a small guanosine-5'-triphosphate (GTP) binding protein that plays a key role in multiple cellular signaling pathways.[1] Activated ROCK phosphorylates the myosin-binding subunit of myosin light chain phosphatase, which inhibits activity of the phosphatase and leads to muscle contraction by regulating the shape and function of the actomyosin complex.[2] Considerable evidence suggests that RhoA/ROCK signaling pathways play an important role in the pathogenesis of multiple diseases, and inhibition of ROCK function and its downstream signaling pathways has the potential to effect a variety of pathological conditions.[3-5] There are two known human ROCK isoforms, ROCK1 and ROCK2, which share 65% overall sequence identity including 92% in the kinase domain. Furthermore, there is 100% identity within the adenosine triphosphate (ATP) binding pocket between the two isoforms.[6] The distinct physiological roles for the individual isoforms continue to be elucidated.

Dual ROCK1/2 inhibitors, which have comparable affinity for ROCK1 and ROCK2, have been approved to treat human diseases. Examples of clinically approved and advanced ROCK inhibitors are shown in Figure 1. Fasudil was marketed for cerebral vasospasm in Japan.[7-8] Ripasudil[9] and Netarsudil[10] (an ester which generates active metabolite AR-13503) have been marketed for glaucoma/ocular hypertension. Pre-clinical studies of the dual ROCK1/2 inhibitor Y-27632 have shown hemodynamic and anti-remodeling effects in animal models.[11] ROCK2 selective inhibitor KD025 (SLx-2119) is being clinically investigated for the potential treatment of multiple diseases.[12-14] However, the dual ROCK1/2 inhibitors lack overall kinome selectivity, and the affinity of KD025 for ROCK2 is modest. Given the potential therapeutic applications, potent and kinome selective dual ROCK inhibitors are of interest. Herein we describe a series of 5*H*-chromeno[3,4-*c*]pyridine, 6*H*-isochromeno[3,4-*c*]pyridine and 6*H*-isochromeno [4,3-*d*]pyrimidine dual ROCK1 and ROCK2 inhibitors.

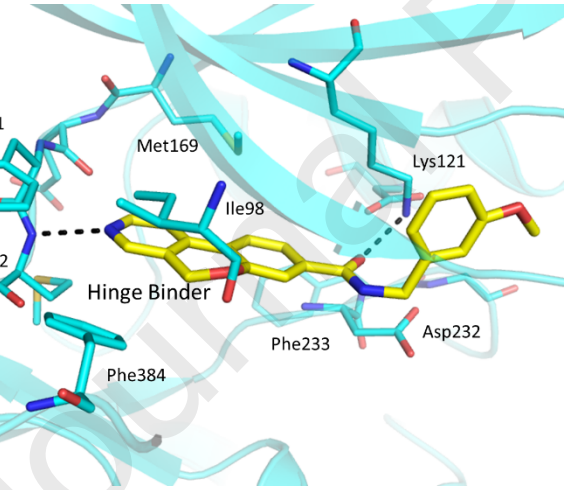

Figure 1. Advanced ROCK inhibitors.

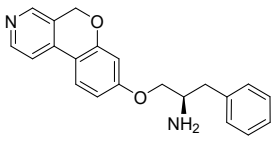

1
ROCK1 IC_{50} 71 nM
ROCK2 IC_{50} 54 nM

Figure 2. An initial lead ROCK inhibitor.

Compound **1** containing the 5*H*-chromeno[3,4-*c*]pyridine moiety was identified as a lead through our internal kinase screening (Figure 2). It demonstrated moderate ROCK1 and ROCK2 affinities with IC_{50} values of 71 nM and 54 nM, respectively. Structure-activity relationship (SAR) optimization on this lead is shown in Table 1. Replacement of the ether with an amide linker, such as (*D*)-phenylalanine derivative **2**, showed moderate improvement in potency. (*D*)-Phenyl glycine homolog **3** further improved ROCK2 potency. Des-amino analog **4**, however, was less potent. To avoid a potential aniline issue, reversing the amide resulted in benzamide **5**, which was similarly potent compared with **4**. Introducing a *meta*-methoxy substitution on the phenyl (**6**) or a benzylic methyl substitution (**7**) improved potency further to single digit nanomolar ROCK2 IC_{50}. Combination of these two substitution groups provided **8** with ROCK1 and ROCK2 IC_{50} values of 13 nM and 0.51 nM, respectively. The corresponding pyridine analog (**9**) retained single digit nanomolar ROCK2 potency; albeit 10-fold less potent for ROCK2.

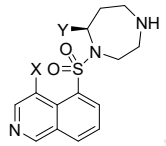

Fasudil (X = H, Y = H)
ROCK1 IC_{50} 940 nM
ROCK2 IC_{50} 220 nM
Ripasudil (X = F, Y = Me)
ROCK1 IC_{50} 50 nM
ROCK2 IC_{50} 20 nM

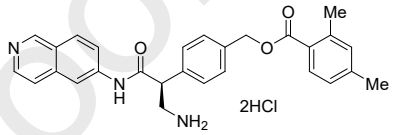

Netarsudil (AR-13324)
ROCK1 K_i 1.0 nM
ROCK2 K_i 1.0 nM
AR-13503 (alcohol metabolite)
ROCK1 K_i 0.2 nM
ROCK2 K_i 0.2 nM

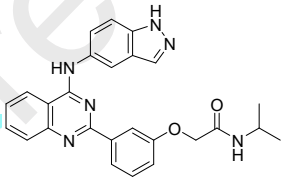

KD025 (SLx-2119)
ROCK1 K_i 24000 nM
ROCK2 K_i 105 nM

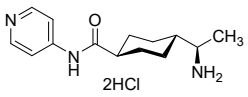

Y-27632
ROCK1 K_i 140 nM
ROCK2 K_i 300 nM

Table 1. SAR of amide linker

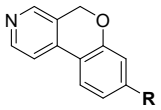

Cpd#	R	IC_{50} (nM)*[15]	
		ROCK1	ROCK2
1	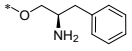	71	54

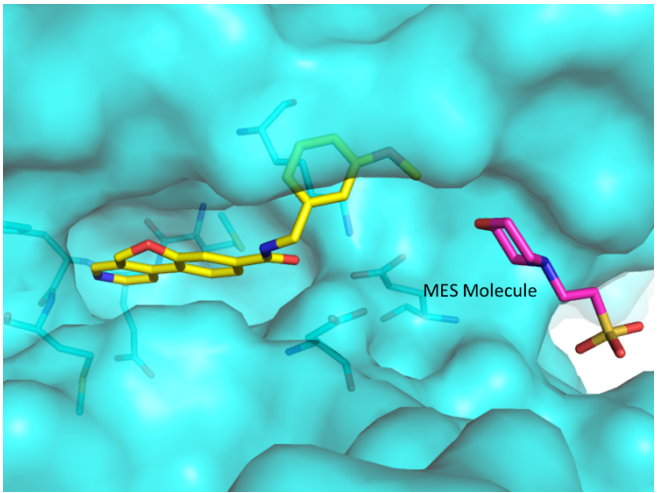

	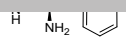		
3	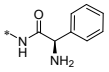	16	9.4
4	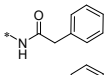	140	44
5	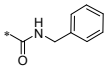	81	29
6	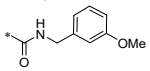	33	6.3
7	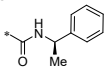	18	3.2
8	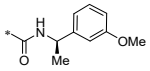	13	0.51
9	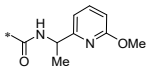	27	6.2

*IC_{50} values listed in Table 1 - 3 are Caliper assay data. See reference 15 for details.

Figure 3. X-ray crystal structure of **6** in ROCK2 (2.55 Å resolution).

An X-ray crystal structure of **6** in ROCK2 was obtained (Figure 3).[16] Compound **6** binds to the ROCK2 active site with DFG-in conformation. The pyridine portion of the 5*H*-chromeno[3,4-*c*]pyridine interacts with the hinge, and the *meta*-methoxyphenyl group tucks under the *p*-loop towards the *c*-helix. The carbonyl oxygen forms a favorable electrostatic interaction with conserved residue Lys121. Electron density in the hinge region indicates that both flips of the tricycle exist in roughly equal probability. In addition, the crystal structure reveals that 2-(*N*-morpholino)ethanesulfonic acid (MES) from the buffer co-crystalized and occupied the space close to the active site near the *c*-helix. The X-ray structural information provided a guide for the possible tolerability of hinge binder modifications and extended substitution groups towards the *c*-helix region (*vide infra*).

Keeping the amide constant, SAR on the tricyclic hinge binder was explored. It was found that the derivative of the regioisomer of 6*H*-isochromeno[3,4-*c*]pyridine (**10**) was more potent for ROCK1 and approximately equal potent for ROCK2 comparing to **8** with ROCK1 and ROCK2 IC_{50} values of 1.2 nM and 0.35 nM, respectively. However, the corresponding benzonaphthyridinones (**11**, **12**) were less potent than **10**, significantly so for **12**, in which the lactam carbonyl may clash electrostatically with the backbone C=O of *p*-loop residue Ile98 based on modeling into the active site. Changing from pyridine to pyrimidine, 6*H*-isochromeno[4,3-*d*]pyrimidine analog **13** retained single-digit nanomolar ROCK2 potency. *Ortho*-amino substitution resulted in 5 and 6-fold reduction in ROCK1 and ROCK2 potencies respectively (**14**). Modeling and the X-ray structure of **6** (Figure 3) indicated that hydrophobic substitutions on the central ring could potentially add affinity via hydrophobic interactions with residue Phe384 at the lip of the hinge binding site. *C*5-Methyl substituted analog **15** (diastereomer mixture) maintained similar ROCK1 potency to compound **8** as less potent for ROCK2. The corresponding regioisomer **16** with *C*6-methyl substitution had excellent potency with sub-nanomolar ROCK1 and ROCK2 IC_{50} values (0.49 nM and 0.21 nM, respectively). Extending to ethyl substitution provided similarly excellent potency (**17**, diastereomer mixture). The two diastereomers in **17** were separated. Both diastereomers showed potent ROCK activities, and diastereomer **19** demonstrated sub-nanomolar ROCK1 and ROCK2 IC_{50} potencies was tolerated.

Table 2. Hinge binder modifications.

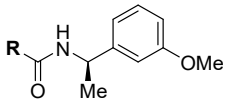

Cpd#	R	IC_{50} (nM)[15] ROCK1	ROCK2
10	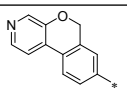	1.2	0.35
11	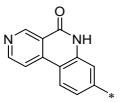	56	14
12	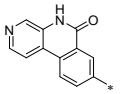	>2000	340
13	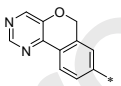	38	2.4
14	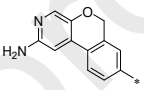	171	16
15	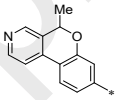	15	4.7
16	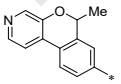	0.49	0.21
17	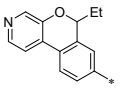	0.63	0.56
18 (isomer 1)	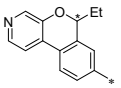	2.0	0.52
19 (isomer 2)	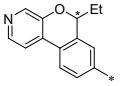	0.67	0.18
20	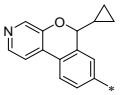	4.1	0.72

The X-ray structure of **6** (Figure 3) indicated there was available binding space near the *c*-helix pocket which could accommodate extended substitution groups. Based on this insight, a series of *meta*-amide analogs were evaluated (Table 3). Amides with increasing size (**21** - **23**) were tolerated, and they exhibited single digit nanomolar or sub-nanomolar IC_{50} values for ROCK1 and ROCK2. Analog **26** with a larger group, (1-ethylpyrrolidin-2-yl)methylamine amide, provided a dual ROCK1 and ROCK2 inhibitor with IC_{50} values of 1.2 nM and 0.5 nM, respectively. These extended groups could be combined with substitutions on the tricyclic hinge binders and provided potent ROCK1 and ROCK2 inhibitors (**24** - **26**).

Table 3. Exploration of extended *c*-helix binding site

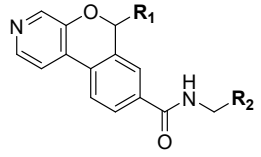

Cpd#	R_1	R_2	ROCK1	ROCK2
21	H	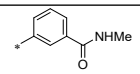	8.0	1.3
22	H	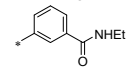	7.0	0.8
23	H	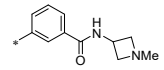	8.9	0.85
24	Me	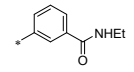	3.2	0.8
25	Et	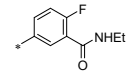	20	3.0
26	Me	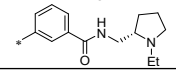	1.2	0.5

*Racemic/diasteromeric mixtures for **24** - **26**

Kinome selectivity of selected compounds was evaluated and the fraction selectivity indices (FSI100, obtained from a kinase panel up to 152 kinases) are listed in Table 4. These ROCK inhibitors exhibited good kinase selectivity. Compound **19** demonstrated excellent ROCK1 and ROCK2 potencies with outstanding kinome selectivity, that no other kinases were inhibited with <100x of ROCK2 IC_{50}.

Table 4. Kinome selectivity indices

Cpd#	**8**	**10**	**19**	**20**	**22**	**23**	**25**
FSI100*	2.6	2.2	1.3	2.0	2.2	5.4	2.2

* Fraction selectivity index is the ratio of active kinases with IC_{50} <100-fold of ROCK2 (including ROCK1/2) out of total tested kinases (up to152 kinases).

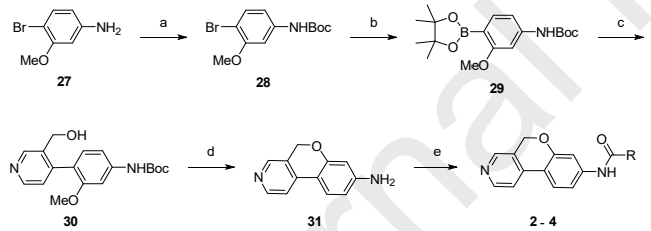

Scheme 1. Reagents and conditions: (a) Boc_2O, TEA, THF, reflux, 80% (b) B_2Pin_2, KOAc, $PdCl_2$(dppf)-DCM adduct, DMF, 100 °C, 12 h, 50% (c) (i) 4-chloronicotinaldehyde, $PdCl_2$(dppf)-DCM adduct, K_3PO_4, dioxane/H_2O, 100 °C, 1 h, 84% (ii) $NaBH_4$, MeOH, 0 °C, 1 h, 98% (d) 63% aq. HBr, 100 °C, 16 h, basic workup, 83% (e) carboxylic acid, T_3P, DIEA, DMF, rt, aq. workup; TFA /DCM treatment for Boc deprotection, 70 - 95%

Compounds **2** - **4** were synthesized according the Scheme 1. *N*-Boc protected 4-bromoaniline **28** was converted to boronate **29**, which reacted with 4-chloronicotinaldehyde under Suzuki coupling conditions, followed by aldehyde reduction, to provide **30**. When **30** was treated with aqueous HBr at elevated temperature, the Boc group was removed, and the methyl ether was cleaved and cyclized with the benzyl alcohol, resulting in 5*H*-chromeno[3,4-*c*]pyridin-8-amine **31**. Amide coupling of **31** with the appropriate carboxylic acids provided **2** - **4**.

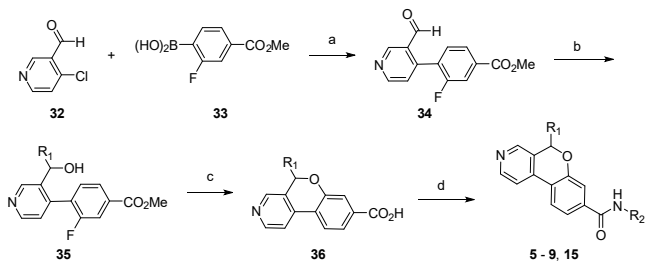

Scheme 2. Reagents and conditions: (a) XPhos-Pd-PreCat-G_2, K_3PO_4, dioxane/H_2O, microwave, 140 °C, 10 min, 58% (b) $NaBH_4$, MeOH, 0 °C, 90% or MeMgBr, THF, 0 °C, 30 min, 68% (c) NaH, THF, 0 - rt, 2 h, then aq. basic treatment, 56% (R_1 = Me) (d) amines, HATU, DIEA, DMF, 40 - 90%

Compounds **5** - **9** and **15** were synthesized by following the procedures in Scheme 2. Suzuki coupling between 4-chloronicotinaldehyde **32** and boronic acid **33** gave aldehyde **34**. Reduction of **34** by $NaBH_4$ provided the primary alcohol, whereas treatment with methyl Grignard reagent provided the secondary alcohol. Cyclization of **35** under S_NAr condition and basic workup provided acid **36**. Amide formation with corresponding amines gave compounds **5** - **9** and **15**.

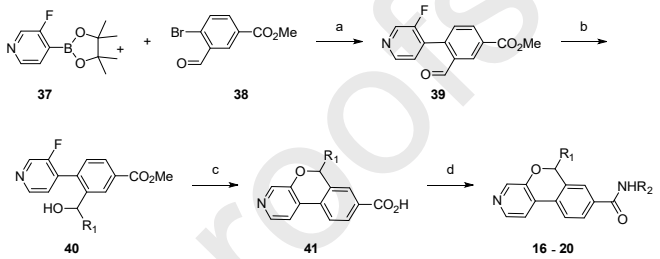

Scheme 3. Reagents and conditions: (a) XPhos-Pd-PreCat-G_2, K_3PO_4, dioxane/H_2O, 2 h, 68% (b) $NaBH_4$, MeOH, 0 °C, 30 min, 52%; or RMgBr (R = Me, Et, cPr), THF, 0 °C - rt, 1 h, 50 - 80% (c) NaH, THF, 0 °C - rt, 16 h, aq. workup, 30-65% (d) amines, HATU, DIEA, DMF, rt, 35 - 85%

The 6*H*-isochromeno[3,4-*c*]pyridine-8-carboxamides **16** - **20** were prepared by following the procedures shown in Scheme 3 using similar chemistry to that described in Scheme 2. Substitutions were introduced from aldehyde **39** when treated with different Grignard reagents before cyclization.

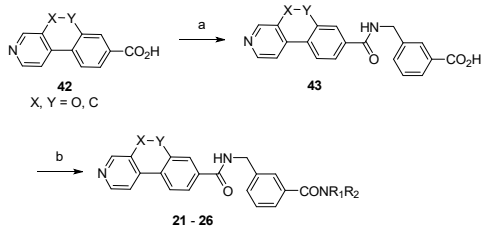

Scheme 4. Reagents and conditions: (a) (i) HATU, DIEA, DMF, rt (ii) NaOH, EtOH/H_2O, rt, 2.5 h, 77% (b) amines, HATU, DIEA, DMF, rt, 45 - 90%

Scheme 4 outlines the synthesis of compounds in Table 3. Intermediates **42** were converted to the corresponding *meta*-ester benzylamide, followed by saponification to afford acids **43**, which were coupled with amines to provide **21** - **26**.

In summary, a novel series of potent and selective dual ROCK1/2 inhibitors were discovered based on the chromenopyridine and chromenopyrimidine hinge-binder scaffolds. Representative inhibitors, such as **19**, demonstrated sub-nanomolar ROCK1/2 IC_{50} values of inhibitory activity with excellent kinome selectivity.

Acknowledgments

We would like to thank Dr. John S. Sack for refining the crystal structure and preparing data for RCSB PDB deposition, and Karen

Ros
ray diffraction data and partially refined crystal structure were obtained from Proteros. BMS Lead Discovery and Optimization generated kinome selectivity data. We appreciate Drs. Heather Finlay, Peter Glunz, Ellen Kick, and Joseph Luettgen for reviewing this manuscript.

References and notes

1. Leung, T.; Manser E.; Tan, L.; Lim, L. *J. Biol. Chem.* **1995**, *270*, 29051-29054.
2. Schofield A. V.; Bernard O. *Crit. Rev. Biochem. Mol. Biol*. **2013**, *48*, 301-316.
3. Knipe, R. S.; Tager, A. M.; Liao, J. K. *Pharmacol. Rev*. **2015**, *67*, 103-117.
4. Loirand, G. *Pharmacol. Rev*. **2015**, *67*, 1074-1095.
5. Feng, Y.; LoGrasso, P. V.; Defert, O.; Li, R. *J. Med. Chem.* **2016**, *59*, 2269-2300.
6. Matsui, T.; Amano, M.; Yamamoto, T.; Chihara, K.; Nakafuku, M.; Ito, M.; Nakano, T.; Okawa, K.; Iwamatsu, A.; Kaibuchi, K. *EMBO J.* **1996**, *15*, 2208-2216.
7. Nagumo, H.; Sasaki, Y.; Ono, Y.; Okamoto, H.; Seto, M.; Takuwa, Y. *Am. J. Phys.- Cell Phys.* **2000**, *278*, C57-65.
8. Naraoka, M., Munakata, A.; Matsuda, N.; Shimamura, N.; Ohkuma, H. *Transl. Stroke Res.* **2013**, *4*, 368-374.
9. (a) Inoue, T.; Tanihara, H. *Expert. Opin. Pharmacther*. **2017**, *18*, 1669-1673. (b) Garnock-Jones, K. P. *Drugs **2014***, *74*, 2211-2215.
10. Lin, C.-W.; Sherman, B.; Moore, L. A.; Laethem, C. L.; Lu, D.-W.; Pattabiraman, P. P.; Rao, P. V.; DeLong, M. A.; Casey C. Kopczynski, C. C. *J. Ocul. Pharmacol. Ther.* **2018**, *34*, 40-51.
11. Cantoni, S.; Pastore, F.; Cavalli, S.; Marchini, G.; Villetti, G.; Nassini, R.; De Logu, F.; Facchinetti, F. *Eur. Respiratory J.* **2016**, *48*, PA5100.
12. Zanin-Zhorov, A.; Weiss, J. M.; Nyuydzefe, M. S.; Chen, W.; Scher, J. U.; Mo, R.; Depoil, D.; Rao, N.; Liu, B.; Wei, J.; Lucas, S.; Koslow, M.; Roche, Maria; Schueller, O.; Weiss, S.; Poyurovsky, M. V.; Tonra, J.; Hippen, K. L.; Dustin, M. L.; Blazar, B. R.; Liu, C.-J; Waksal, S. D. *Proc. Nat. Acad. Sc. USA* **2014**, *111*, 16814-16819.
13. Park, J.; Chun, K.-H. *Gene*, **2020**, *737*, 144474.
14. KD025 - Clinical Trials, *ClinicalTrials.gov,* NCT03919799, December 20, **2019**.
15. Caliper Assay: *In vitro* potencies of ROCK inhibitors were determined in an assay containing 20 mM HEPES, pH 7.5, 20 mM $MgCl_2$, 0.015% Brij-35, 4 mM DTT, 5 µM ATP and 1.5 µM peptide substrate (FITC-AHA-AKRRRLSSLRA-OH, Tufts University, final concentration of DMSO was < 2%, and the reaction was initiated with ROCK1 or ROCK2 produced at BMS. After incubation, the reaction was terminated by the addition of EDTA and the phosphorylated and non-phosphorylated peptides separated using a LabChip 3000 Reader (Caliper Life Sciences). Controls consisted of assays that did not contain compound, and backgrounds consisted of assays that contained enzyme and substrate but had EDTA from the beginning of the reaction to inhibit kinase activity. Compounds were tested in dose-response format, and the inhibition of kinase activity was calculated at each concentration of compound. The inhibition data were fit to a four-parameter logistic equation y = A+((B-A)/(1+((C/x)^D))), where A and B denote minimal and maximal % inhibition, respectively, C is the IC_{50}, D is hill slope and x represents compound concentration equation, to determine the IC_{50}; i.e., the concentration of compound required to inhibit 50% of kinase activity. Potencies of ROCK inhibitors were also determined in homogeneous time-resolved fluorescence (HTRF assay), a time resolved FRET-based competition binding assay. A His-tagged form of ROCK1 or ROCK2 produced at BMS at a concentration of 1 nM was incubated with 0.2 nM Tb-labeled anti-His detection antibody (Cis-Bio, MA), test compound, and fluorescein-labeled ATP competitive probe at a concentration corresponding to the probe's equilibrium dissociation constant for one hour. Fluorescence at 495 nm and 520 nm was measured using an EnVision microplate reader to quantify FRET between Tb-labeled detection antibody and fluorescein-labeled probe. Background subtracted FRET ratios were normalized to the maximum signal obtained in the absence of test compound. These values were converted to a percent inhibition. Percent inhibition was determined for test compounds at 11 concentrations. The IC50, defined as the concentration of competing test compound needed to reduce specific binding of the probe by 50%, was derived by fitting data to the 4-parameter logistic equation y = A+((B-A)/(1+((C/x)^D))), where A and B denotes minimal and maximal % inhibition, respectively, C is the IC50, D is hill slope and x represents compound concentration. ROCK1 and ROCK2 potencies were determined by both methods. The potencies of the other kinases in the kinase panel for selectivity were determined using either of the two methods.
16. The PDB ID is 7JNT.